

See discussions, stats, and author profiles for this publication at: <https://www.researchgate.net/publication/231274912>

# Global Rate Expression for Nitric Oxide Reburning. Part 2

ARTICLE *in* ENERGY & FUELS · SEPTEMBER 1996

Impact Factor: 2.79 · DOI: 10.1021/ef960007v

---

CITATIONS

42

---

READS

19

4 AUTHORS, INCLUDING:



Thomas H. Fletcher

Brigham Young University - Provo Main Cam...

155 PUBLICATIONS 2,290 CITATIONS

SEE PROFILE

# Global Rate Expression for Nitric Oxide Reburning. Part 2

W. Chen,<sup>†</sup> L. D. Smoot,\* S. C. Hill,<sup>‡</sup> and T. H. Fletcher<sup>§</sup>

Advanced Combustion Engineering Research Center, Brigham Young University,  
Provo, Utah 84602

Received January 11, 1996<sup>®</sup>

An investigation of a global reburning-NO reaction,  $\sum_i C_i H_j + \text{NO} \rightarrow \text{HCN} + \dots$ , which is a reduction pathway of nitric oxide (NO) by reaction with gaseous hydrocarbons, was conducted. The global reburning-NO rate expression was deduced from a combination of elemental reactions. The global rate expression and its rate constants were then determined by correlating predicted species profiles from simple hydrocarbon flames. This global reburning-NO rate constant can be expressed as  $2.7 \times 10^6 \exp(-18\,800/RT)$  (gmol/cm<sup>3</sup> s). This expression and constants are applicable to atmospheric pressure with an equivalence ratio range of 1.0–2.08 for light hydrocarbon reburning gases (CH<sub>4</sub> and C<sub>2</sub>H<sub>4</sub>).

## Introduction

Coal combustion is a major source of nitric oxide and nitrogen dioxide, namely NO<sub>x</sub>, with at least 33% of man-made NO<sub>x</sub> thought to be generated from this source.<sup>1,2</sup> Coal combustion in a furnace or a reactor consists of several steps such as coal devolatilization, gaseous combustion, and heterogeneous oxidation of char. During combustion, elemental nitrogen (N) bound in coal, called fuel-N, and molecular nitrogen (N<sub>2</sub>) in air are oxidized to form NO<sub>x</sub>. NO<sub>x</sub> typically consists of 95% NO, together with small amounts of NO<sub>2</sub>, and N<sub>2</sub>O.<sup>3,4</sup>

Study of the formation and destruction processes of NO<sub>x</sub> is substantially aided by computer modeling.<sup>5</sup> In a turbulent environment, the technology does not exist for realistically performing these computations with a fundamental reaction mechanism comprising hundreds of reactions. Hence, a global chemistry approach, emphasizing major chemical species and reactions, has been commonly used<sup>5,6</sup> in the calculation of pollutant concentrations.

The fuel-NO mechanism is dominant in the formation of NO during coal combustion, and various global fuel-NO rate expressions and coefficients have been published.<sup>7–9</sup> The conversion of fuel-N to NO has commonly

been observed to be incomplete, especially under fuel-rich conditions. Several elementary reaction steps have been suggested to describe this low conversion.<sup>10–14</sup> These elementary steps include what is called the “reburning-NO mechanism”. This reaction can be expressed globally as  $\text{NO} + \text{C}_i \text{H}_j \rightarrow \text{HCN} + \dots$ , where C<sub>i</sub>H<sub>j</sub> is the pool of gaseous hydrocarbon species.

The reburning-NO mechanism is important in environments rich in hydrocarbon radicals.<sup>15–18</sup> Coal combustion usually occurs in a diffusion flame, as combustible gases are released from coal and then mix and react with the oxygen in the bulk stream. In fuel-rich

(7) De Soete, G. C. Overall reaction rates of NO and N<sub>2</sub> formation from fuel nitrogen. *Fifteenth Symposium (International) on Combustion*; The Combustion Institute, Pittsburgh, PA, 1975; p 1093.

(8) Mitchell, J. W.; Tarbell, J. M. A kinetic model of nitric oxide formation during pulverized coal combustion. *AIChE J.* **1982**, *28*, 302.

(9) Bose, A. C.; Wendt, J. O. L. Effects of coal composition on mechanisms governing the destruction of nitrogenous species during staged combustion. *Western States Section/Combustion Institute*, Honolulu, HI, 1987; p 114.

(10) Wendt, J. O. L.; Sternling, C. V.; Matovich, M. A. Reduction of sulfur trioxide and nitrogen oxides by secondary fuel injection. *Fourteenth Symposium (International) on Combustion*; The Combustion Institute: Pittsburgh, PA, 1973; p 897.

(11) Myerson, A. L. The reduction of nitric oxide in simulated combustion effluents by hydrocarbon-oxygen mixtures. *Fifteenth Symposium (International) on Combustion*; The Combustion Institute: Pittsburgh, PA, 1975; p 1085.

(12) Song, Y. H.; Blair, D. W.; Simnski, V. J.; Bartok, W. Conversion of fixed nitrogen to N<sub>2</sub> in rich combustion. *Eighteenth Symposium (International) on Combustion*; The Combustion Institute: Pittsburgh, PA, 1981; p 53.

(13) Chen, S. L.; McCarthy, J. M.; Clark, W. D.; Heap, M. P.; Seeker, W. R.; Pershing, D. W. Bench and pilot scale process evaluation of reburning for in-furnace NO<sub>x</sub> reduction. *Twenty-First Symposium (International) on Combustion*; The Combustion Institute: Pittsburgh, PA, 1986; p 1159.

(14) Wornatz, M. J.; Sarofim, A. F.; Longwell, J. P. Pyrolysis-induced changes in the ring number composition of polycyclic aromatic compounds from a high volatile bituminous coal. *Twenty-Second Symposium (International) on Combustion*; The Combustion Institute: Pittsburgh, PA, 1988; p 135.

(15) Westenberg, A. A. Kinetics of NO and CO in lean, premixed hydrocarbon air flows. *Combust. Sci. Technol.* **1971**, *4*, 59.

(16) Hayhurst, A. N.; Vince, I. M. Nitric oxide formation from N<sub>2</sub> in flames: the importance of prompt NO. *Prog. Energy Combust. Sci.* **1980**, *6*, 35.

(17) Miller, J. A.; Bowman, C. Mechanism and modeling of nitrogen chemistry in combustion. *Prog. Energy Combust. Sci.* **1989**, *15*, 287.

(18) Bowman, C. T. Chemistry of gaseous pollutant formation and destruction. In *Fossil Fuel Combustion: A Source Book*; Bartok, W., Sarofim, A. F., Eds.; Wiley: New York, 1991.

<sup>†</sup> Present address: ABB/CE, Windsor, CT.

\* Director and Professor, Chemical Engineering. Author to whom correspondence should be addressed [telephone (801) 378-8930; fax (801) 378-6033].

<sup>‡</sup> Combustion Computations Laboratory.

<sup>§</sup> Chemical Engineering and ACERC.

<sup>®</sup> Abstract published in *Advance ACS Abstracts*, July 1, 1996.

(1) Wark, K.; Warner, C. F. *Air Pollution: Its Origin and Control*; Harper Collins Publisher: New York, 1981.

(2) Babcock & Wilcox. *Steam, Its Generation and Use*; Wiley: New York, 1993.

(3) Merryman, E. L.; Levy, A. Nitrogen oxide formation in flames: the roles of NO<sub>2</sub> and fuel nitrogen. *Fifteenth Symposium (International) on Combustion*; The Combustion Institute: Pittsburgh, PA, 1974; p 1073.

(4) Muzio, L. J.; Montgomery, T. A.; Samuelsen, G. S.; Kramlich, J. C.; Lyon, R. K.; Kokkinos, A. Formation and measurement of N<sub>2</sub>O in combustion systems. *Twenty-Third Symposium (International) on Combustion*; The Combustion Institute: Pittsburgh, PA, 1990; p 245.

(5) Smoot, L. D.; Smith, P. J. *Coal Combustion and Gasification*; Plenum Press: New York, 1985.

(6) Lockwood, F. C.; Yeshia, M. A. Simulation of pulverized coal test furnace performance. *Twenty-Fourth Symposium (International) on Combustion (Poster)*; The Combustion Institute: Pittsburgh, PA, 1992.

regions, with relatively high hydrocarbon radical concentrations, the reburning-NO mechanism becomes significant. In addition, a practical abatement technology for reducing  $\text{NO}_x$  emissions relies on the aft injection of a hydrocarbon such as methane to reduce NO to HCN through the *reburning reaction*. However, a global rate expression for reburning-NO, suitable for engineering design, has not been reported in the literature.

Commonly, the rate constants of a global mechanism are correlated empirically from experimental data (e.g., De Soete<sup>7</sup>). Since the reburning-NO mechanism depends strongly upon hydrocarbon radicals, which are difficult to measure, the global reburning-NO mechanism cannot be readily obtained in this manner. In this research, an analytical method, reported in part 1 of this study,<sup>19</sup> has been applied to deduce a global mechanism systematically from a comprehensive set of elementary chemical kinetic steps.<sup>20</sup> By this method, a global reburning-NO rate expression is derived, and comprehensive predictions of species profiles in premixed flames are used to evaluate the global rate constants.

### Methodology

With known species concentration profiles, three methods for deriving global rate expressions have been applied by various investigators. First, the formation path is postulated and rate expressions are determined from measured species concentrations.<sup>7,21</sup> Second, from a postulated set of global mechanisms, where rate constants are known for most but not all reactions, missing rate constants are deduced from overall predictive fits of measured data.<sup>8</sup> Third, by compilation of all relevant elementary chemical reactions, rate-determining reactions are identified, global rate expressions are deduced from these rate-determining reactions, and rate constants are determined from predicted species profiles.<sup>19</sup> The third approach has been used in this research. Because of the difficulties in measuring radical concentrations and limited experimental information, along with the rapid progress in the development of full kinetic mechanisms, the third approach can be the preferred choice in the determination of global reaction mechanisms and corresponding rate constants.

A reaction scheme with 254 gaseous elementary reactions was used for simulations of NO formation in premixed, laminar hydrocarbon-containing flames, together with the CHEMKIN code.<sup>22</sup> Of these 254 steps, 234 reactions are from Miller and Bowman,<sup>17</sup> The balance are from Tables 2 and 3 in Zabarnick,<sup>23</sup> which add  $\text{NO}_2$  and  $\text{N}_2\text{O}$  reaction steps. Rate constants used for this study were reported by Zabarnick et al.,<sup>24</sup> Miller and Bowman,<sup>17</sup> and Zabarnick.<sup>23</sup> A complete listing of these rate constants is given by Chen.<sup>20</sup>

In this work, a global reburning-NO rate expression is deduced and rate constants are correlated from predicted species profiles for premixed hydrocarbon flames. The global

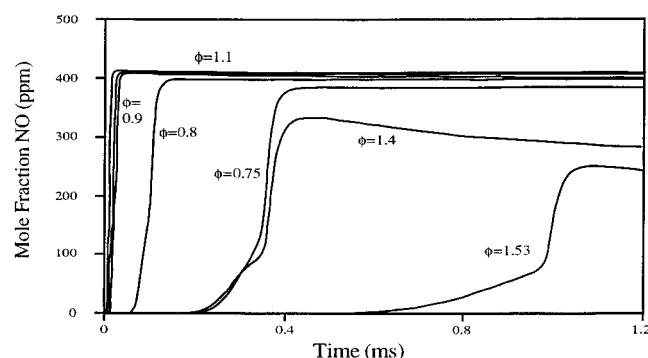


**Figure 1.** Effect of equivalence ratio on predicted NO concentration in premixed flames. Conditions:  $\text{C}_2\text{N}_2$ , 200 ppm;  $\text{C}_2\text{H}_4/\text{O}_2/\text{Ar}$  at atmospheric pressure; flame conditions from De Soete.<sup>7</sup>

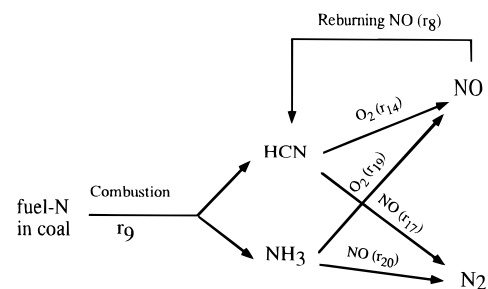


**Figure 2.** Overall fuel-N to NO reaction pathway.

reburning-NO rate constant is closely coupled with two other global rate constants for NO production from fuel-N. These other two global rate constants were also correlated by this method and compared with the rate constants measured by De Soete<sup>7</sup> as a means to verify the method. The methodology for obtaining global rate constants from full mechanism predictions and verification by reproducing De Soete's global rate constants for fuel-N have been reported in a companion paper.<sup>19</sup> A discussion of the validity of the global reburning-NO rate expression and its constants is presented in this paper.

### Rate-Determining Reactions

**Nitrogen Reactions.** Nitrogen reactions include the reactions that form or destroy NO, HCN, and  $\text{NH}_3$ . It is well-known that NO formation from the thermal-NO mechanism and the prompt-NO mechanism is typically small or negligible in coal-fired systems compared with NO from the fuel-NO pathway. NO formation varies with equivalence ratio, with the maximum NO conversion occurring near stoichiometric conditions.

Figure 1 shows predicted concentration profiles of NO from the CHEMKIN code<sup>22</sup> with different equivalence ratios in premixed, laminar  $\text{C}_2\text{H}_4$  flames. In these simulations, the fuel-N compound,  $\text{C}_2\text{N}_2$ , has the same initial concentration (220 ppm) while the  $\text{C}_2\text{H}_4/\text{oxygen}$  ratios are varied. In fuel-lean combustion ( $\phi < 1.0$ ), NO has high formation rates in the flame and then remains at near-maximum values. In near-stoichiometric combustion, NO formation starts early, principally by conversion of fuel-N. In fuel-rich combustion ( $\phi > 1.0$ ), the formation process becomes more complex, and a region of slow NO formation exists, followed by a high formation region. This high formation is followed by the destruction of HCN. Once NO values peak, significant NO reduction occurs. The NO profiles suggest a significant difference in the NO reaction mechanisms in fuel-rich vs fuel-lean flames.

The existence of fuel-N dominates the overall NO formation pathway. However, in the post-flame region,

(19) Chen, W.; Smoot, L. D.; Fletcher, T. H.; Boardman, R. D. A computational method for determining global fuel-NO rate expressions. Part 1. *Energy Fuels* **1996**, *10*, 1036.

(20) Chen, W. A global rate of nitric oxide reburning. Ph.D. Dissertation, Department of Chemical Engineering, Brigham Young University, Provo, UT, 1994.

(21) Bose, A. C.; Dannecker, K. M.; Wendt, J. O. L. Coal combustion effects on mechanisms governing the destruction of NO and other nitrogenous species during fuel-rich combustion. *Energy Fuels* **1988**, *2*, 301.

(22) Kee, R. J.; Rupley, F. M.; Miller, J. A. Chemkin-II: A FORTRAN chemical kinetics package for the analysis of gas-phase chemical kinetics. SANDIA Report, SAND89-8009. UC-401, Livermore, CA, March 1991.

(23) Zabarnick, S. A comparison of  $\text{CH}_4/\text{NO}/\text{O}_2$  and  $\text{CH}_4/\text{N}_2\text{O}$  flames by LIF diagnostics and chemical kinetic modeling. *Combust. Sci. Technol.* **1992**, *83*, 115.

(24) Zabarnick, S.; Fleming, J. W.; Lin, M. C. Kinetics of CH radical reactions with propane, isobutane and neopentane. *Chem. Phys.* **1987**, *112*, 409.

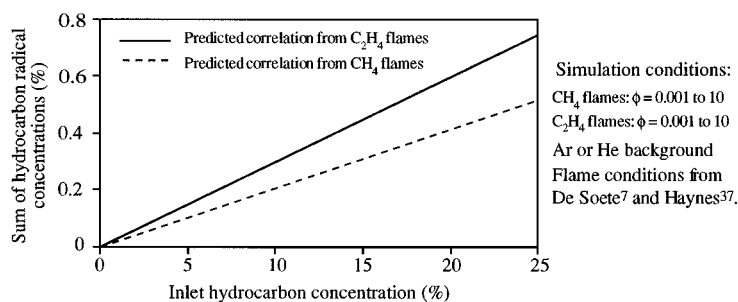
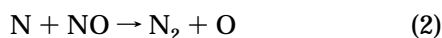
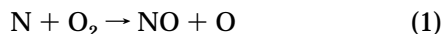
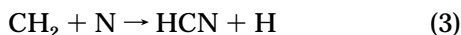


**Figure 3.** Predicted dependence of hydrocarbon radical concentrations in the premixed flame reaction zone on inlet hydrocarbon concentrations from simulations. Reaction zone for this correlation is identical to that for deduction of the global reburning rate correlation, namely when 90% of the fuel-N has been depleted.

the thermal-NO mechanism is significant, especially the reactions:



The prompt-NO mechanism, for example



is not important in the formation of NO in fuel-lean flames. Thermal NO reactions 1 and 2 are dominant in the absence of fuel-N, while the prompt-NO step (reaction 3) is negligible. The reburning steps (for example,  $\text{CH}_2 + \text{NO} \rightarrow \text{HCN} + \text{OH}$ ) are also not significant in fuel-lean flames.

The hydrocarbon radicals such as CH and  $\text{CH}_2$  react with NO:



The intermediate HCNO is reduced to HCN through the step



These reburning-NO steps can be summarized as a global step in the following form:



where  $i = 1, 2$ , or 3 and higher, depending on the hydrocarbons used in the flames.

$\text{NH}_3$  is another major nitrogen species formed from fuel-N, and it is oxidized to NO during combustion.<sup>25</sup> From the simulations of both fuel-lean and fuel-rich flames with  $\text{C}_2\text{N}_2$  as fuel-N, negligible  $\text{NH}_3$  concentrations were predicted, which may imply that  $\text{C}_2\text{N}_2$  does not readily convert to  $\text{NH}_3$ . Solomon et al.<sup>26</sup> observed that a significant amount of  $\text{NH}_3$  was generated from coal-char particles in a reducing atmosphere in a TGA, which may indicate that  $\text{NH}_3$  may be directly converted from fuel-N or through char-fuel-N reactions. In other words, fuel-N from coal may produce both  $\text{NH}_3$  and HCN, but HCN does not directly convert to  $\text{NH}_3$ . Hence, premixed flames have been simulated to study

the significance of reburning-NO steps when  $\text{NH}_3$  is used as fuel-N.

With  $\text{NH}_3$  as fuel-N, HCN is generated after significant NO has formed in a fuel-rich flame. This observation indicates that most of the HCN from NO occurs through reburning-NO steps. Therefore, as illustrated in Figure 2, the global NO formation pathway in a fuel-rich  $\text{NH}_3$  flame can be assumed to be  $\text{NH}_3 \rightarrow \text{NO} \rightarrow \text{HCN} \rightarrow \text{NO}$  or  $\text{N}_2$ , which was suggested by Dasch and Blint<sup>27</sup> and Davidson et al.<sup>28</sup>

**Hydrocarbon Reactions.** Figure 3 shows that the predicted sum of hydrocarbon radicals ( $\text{CH}_2$ , CH, etc.) is almost linearly proportional to the inlet hydrocarbon concentration (e.g.,  $\text{CH}_4$ ), for the defined reaction zone of the premixed flames computed in this investigation. This observation is important in application of the global reburning rate, deduced from premixed gaseous hydrocarbon flames, to coal-containing diffusion flames. In fuel-rich devolatilization zones of pulverized-coal diffusion flames, the principal equilibrium hydrocarbon species are compounds such as  $\text{CH}_4$  and  $\text{C}_2\text{H}_4$ .<sup>29</sup> However, in premixed flames, the major nonequilibrium hydrocarbon species in the flame zone (i.e., after 90% of fuel nitrogen is depleted) are CH and  $\text{CH}_2$ . The slope of this linear relationship provides the required constant for estimating the hydrocarbon radical concentrations locally in a diffusion flame, where only the major hydrocarbon concentrations are known.

**Radical Reactions.** The global fuel-NO, thermal-NO, and reburning-NO rates are directly related to the oxygen radical concentration.<sup>30</sup> However, De Soete<sup>7</sup> observed that the global dependence of NO formation on  $\text{O}_2$  is not linear. In other words, the global NO formation rate expression is not first order in the  $\text{O}_2$  concentration. In thermal-NO, the oxygen radical is sometimes assumed to be in equilibrium with the oxygen molecule<sup>31</sup> to calculate NO formed through the thermal-NO steps such as eqs 1 and 2. Estimating the dependence of the oxygen radical on molecular oxygen is difficult in experiments, because accurate measurement of the oxygen radical is difficult. However, it is relatively easy to use computer simulations for such comparisons and investigations.

(27) Dasch, C. J.; Blint, R. J. A mechanistic and experimental study of ammonia flames. *Combust. Sci. Technol.* **1984**, *41*, 223.

(28) Davidson, D. F.; Hoinghaus, K. K.; Chang, A. Y.; Hanson, R. K. A pyrolysis mechanism for ammonia. *Int. J. Chem. Kinet.* **1990**, *22*, 513.

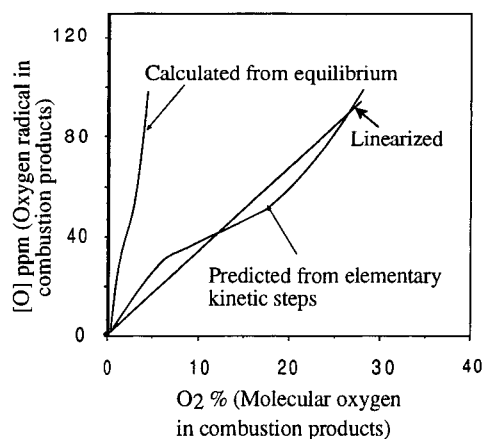
(29) Eaton, A. M.; Hill, S. C.; Brewster, B. S. *User's Manual 93-PCGC-3: Pulverized Coal Gasification or Combustion (3-Dimensional)*; Brigham Young University: Provo, UT, 1993.

(30) Tuazon, E. C.; Atkinson, R. A product study of the gas-phase reaction of isoprene with the OH radical in the presence of  $\text{NO}_x$ . *Int. J. Chem. Kinet.* **1990**, *22*, 1221.

(31) Boardman, R. D. Development and evaluation of a combined thermal and fuel nitric oxide predictive model. Ph.D. Dissertation, Department of Chemical Engineering, Brigham Young University, Provo, UT, 1990.

(25) Bian, J.; Vandooren, J.; Van Tiggelen, P. J. Experimental study of this structure of an ammonia-oxygen flame. *Twenty-First Symposium (International) on Combustion*; The Combustion Institute: Pittsburgh, PA, 1986; p 953.

(26) Solomon, P. R.; Serio, M. A.; Carnagelo, R. M.; et al. Analysis of the Argonne premium coal samples by thermogravimetric Fourier transform infrared spectroscopy. *Energy Fuels* **1990**, *4*, 319.



Simulation conditions:

Equivalence ratio ( $\phi$ ) 0.7 to 1.2  
 Residence time (t) 2 ms  
 Ar 56.4 to 79.2 %  
 Atmospheric pressure

**Figure 4.** Dependence of oxygen radical concentration on oxygen molecule concentration from simulations of ethylene–air flames.

Figure 4 presents a comparison of the equilibrium oxygen radical concentrations and the [O] concentrations from CHEMKIN simulations for  $C_2H_4$ – $O_2$  flames. The equilibrium [O] concentration based on the oxygen molecule concentration is much higher than the non-equilibrium values obtained from the simulations. However, a near-linear relationship between the molecular oxygen concentration and the [O] concentration from the CHEMKIN simulations exists. This observation provides the basis for an improved correlation between  $O_2$  and oxygen radical concentrations for calculating thermal  $NO_x$  in complex, turbulent systems.

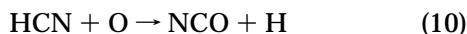
### Global Reburning Nitric Oxide Reaction

The reburning-NO steps are important and sometimes rate-determining in the formation and destruction of NO in hydrocarbon-rich regions of flames.<sup>20</sup> Apparently, without the reburning-NO steps, the simulations of NO formation will result in inaccurate profiles of NO, HCN, and  $NH_3$  in these fuel-rich hydrocarbon flames. In this section, a global reburning NO rate expression is formulated on the basis of the relevant elementary steps, and the coefficients are deduced from predicted species profiles.

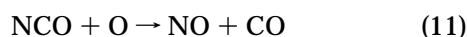
**Reburning Nitric Oxide Pathway.** In the simulations herein,  $C_2N_2$  and  $NH_3$  were used as fuel-N. HCN is observed very early in the flame, and its oxidation results in the formation of NO. Thus, HCN is an intermediate between fuel-N and NO, which connects the fuel-NO and reburning-NO steps. The following global reaction from fuel-N to HCN has been commonly identified:<sup>7,21</sup>



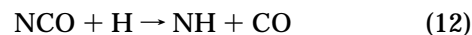
HCN formed from fuel-N can be oxidized further to NO or  $N_2$ .<sup>7,17,21,32</sup> The reaction pathway of HCN can include the following steps:



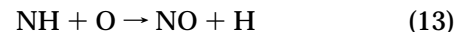
and



or



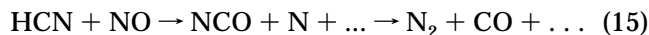
and then



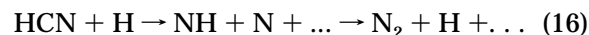
The above steps can be condensed to a global oxidation reaction by including  $O_2 + H \leftrightarrow O + OH$  and  $O_2 + M \leftrightarrow O + O + M$  reactions:



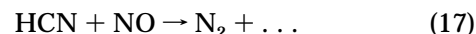
The conversion of HCN can also form NCO, HCNO, and  $NH_i$  radicals by the following pathways:



and



Similar to the global HCN oxidation pathway, the global HCN reduction pathway can be written as follows:



The global rate constants for reaction 17 were also reported by De Soete,<sup>7</sup> on the basis of correlations of laboratory data. The rate constants were also obtained independently by Chen et al.<sup>19</sup> from correlation of computer simulations of hydrocarbon flames.

In fuel-rich flames, the reburning-NO pathway becomes significant, and its global reaction can be generalized from (8) as:

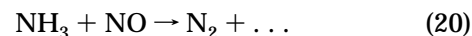


$\sum_{i,j} C_i H_j$  is taken to include all hydrocarbon species which occur locally in the flame zone. In this work, these species included  $C_2H_4$ ,  $C_2H_3$ ,  $C_2H_2$ ,  $C_2H$ ,  $CH_4$ ,  $CH_3$ ,  $CH_2$ , and  $CH$ . However, throughout the simulations in this study, only  $CH$  and  $CH_2$  were predicted in significant concentrations, which was also observed experimentally by Wendt and Mereb.<sup>33</sup>

When  $NH_3$  is used as fuel-N, similar oxidation pathways of  $NH_3$  to NO and  $N_2$  can be obtained analogous to reactions 14 and 17 and have been written in the following forms:<sup>34</sup>



and



The rate constants of the global reactions 19 and 20 were also reported by De Soete<sup>7</sup> from correlation of laboratory data.

**Interactions among NO Mechanisms.** NO formed in a hydrocarbon flame may originate from thermal-NO, fuel-NO, and prompt-NO pathways and may be reduced by HCN reduction and reburning-NO pathways. The

(32) Kramlich, J. C.; Seeker, W. R.; Sarofim, A. F.; Ham, D.; Lester, T. W.; Wendt, J. O. L. *Kinetics of Sulfur and Nitrogen Reactions in Combustion Systems: Vol. I—Project Overview and Narrative*; DOE/PC/70771-T10 (Vol. 1) (DOE91002623); EER: Irvine, CA, Dec 1989.

(33) Wendt, J. O. L.; Mereb, J. B. Nitrogen oxide abatement by distributed fuel addition. DOE Final Report, DE-AC22-87PC79850, University of Arizona, Tucson, AZ, Sept 1991.

(34) De Soete, G. C. Mechanisms of nitric oxides from ammonia and amines in hydrocarbon flames (Le Mechanisme de Formation d'Oxyde Azotique A Partir d'Ammoniac et d'Amines dans les Flammes d'Hydrocarbures). *Rev. Pet. Inst Fr.* **1973**, 28, 171.

fuel-N global reaction sequence is expressed in Figure 2. Rigorously speaking, correlation of reburning-NO should exclude the effects of thermal-NO and prompt-NO. However, as shown in the simulations of Chen,<sup>20</sup> these mechanisms are strongly coupled; hence, it is extremely difficult to separate NO formed from thermal-NO and prompt-NO from the other NO reaction processes.

NO from both thermal-NO and prompt-NO mechanisms is of the order of several to several tens of parts per million. However, NO from fuel-N is usually several hundred parts per million. Often, in coal combustion, the pathways of thermal-NO and prompt-NO are negligible compared to NO from fuel-N. However, in post-flame regions, fuel-N, hydrocarbon radicals, and HCN have already been consumed and flame temperatures are usually still high. In a diffusion flame, oxygen from primary or secondary inlets exists with other exhaust gases. Thus, the oxygen-rich environment and high temperatures create conditions for thermal-NO formation. Therefore, in post-flame regions, NO formed from the thermal-NO mechanisms may not be negligible, especially in a diffusion flame. However, in most of the simulations, the residence time of exhaust gases is relatively short (less than 2 ms), and NO from the thermal-NO mechanism is still small.

In addition to the prompt-NO and thermal-NO mechanisms, some reactions convert fuel-N to NO directly without going through HCN intermediates, such as CN, NH<sub>2</sub>, and N<sub>2</sub>O. Obviously, the determination of these side-paths is even more difficult because some NH<sub>2</sub> or N<sub>2</sub>O may be produced from HCN. Here, a method based on simulations is used to quantitatively evaluate the global reburning-NO pathway. From eq 8 and Figure 2, the global reburning-NO rate  $r_8^{\text{NO}}$ , in the absence of NH<sub>3</sub> reactions, thermal-NO, and prompt-NO, can be expressed, by material balance as

$$r_8^{\text{NO}} = r_{14} - (dX_{\text{NO}}/dt) - r_{17} \quad (21)$$

From Figure 2, the global reburning-NO rate  $r_8^{\text{HCN}}$  can also be written by the same method as

$$r_8^{\text{HCN}} = dX_{\text{HCN}}/dt + r_{14} + r_{17} - r_9 \quad (22)$$

Theoretically, the rates  $r_8^{\text{NO}}$  and  $r_8^{\text{HCN}}$  must be the same if reburning-NO is the only major sink of NO in a fuel-rich flame, and either could be used to determine  $k_8$ . In other words, the ratio of eqs 21 and 22 should be close to unity when reburning is important, and this result can be written in the following form, when the fuel-N is C<sub>2</sub>N<sub>2</sub>. The derivation of eq 23 makes use of eqs 9 and 17, where  $r_9 = -2dX_{\text{C}_2\text{N}_2}/dt$  and  $r_{17} = +2dX_{\text{N}_2}/dt$ :

$$\frac{r_8^{\text{NO}}}{r_8^{\text{HCN}}} = \frac{r_{14} - \frac{dX_{\text{NO}}}{dt} - r_{17}}{\frac{dX_{\text{HCN}}}{dt} + 2\frac{dX_{\text{C}_2\text{N}_2}}{dt} + 2\frac{dX_{\text{N}_2}}{dt} + r_{14}} \approx 1 \quad (23)$$

If C<sub>2</sub>N<sub>2</sub> is assumed to be used as fuel-N, N<sub>2</sub> and NO are the major final products. When NO is seeded into a flame, the term  $r_9$  in eq 22 is then eliminated because there is no primary fuel-N to form HCN.

The ratio  $r_8^{\text{NO}}/r_8^{\text{HCN}}$  was calculated from the complete elementary mechanism using eq 23, and is shown in Figure 5. This ratio is close to unity when the flames

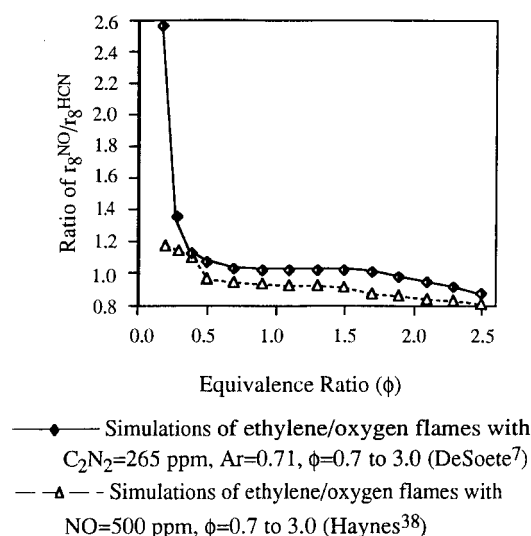
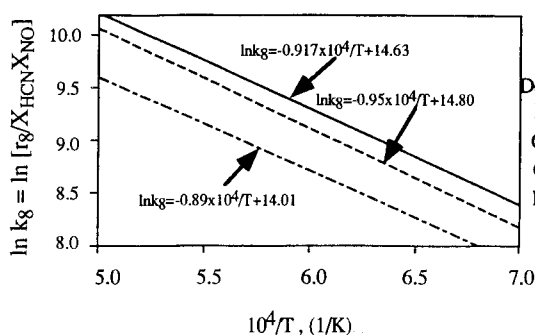


**Figure 5.** Global rate ratio for reaction 8 based on NO to that based on HCN.

become fuel-rich ( $\phi > 1.0$ ). The calculations for fuel-N flames show that the ratio is much higher than unity in these flames for fuel-lean conditions. This could happen with either a lower  $r_8^{\text{HCN}}$  or a higher  $r_8^{\text{NO}}$ . As noted, thermal-NO and prompt-NO are not usually significant when substantial fuel-N exits, although thermal-NO may be higher because of the increased oxygen concentration. Because of the excess oxygen in a fuel-lean flame, the oxidation of HCN may be faster than in a fuel-rich flame, and  $r_8^{\text{HCN}}$  would be lower in a fuel-lean flame. In Figure 5, the bottom curve, which represents the plot of eq 23 with NO seeding, shows that the  $r_8^{\text{NO}}/r_8^{\text{HCN}}$  ratio is close to unity in both fuel-lean and fuel-rich flames. This result implies that the reburning-NO mechanism may be important in both fuel-lean and fuel-rich flames with NO seeding.

### Global Nitric Oxide Reburning Rate Constants

The method used herein for determining  $r_8$  and  $k_8$  by eq 21 or 22 was identical to that used by De Soete<sup>7,34</sup> for the rate constants of eqs 14, 17, 19, and 20, with one exception. He determined mole fractions and their spatial derivatives from test data, whereas in this study the values were taken from calculated mole fraction profiles of one-dimensional, premixed flames. De Soete<sup>7</sup> evaluated the rate constants after the reactant (fuel-N) was mostly consumed. In this work, fuel-N was considered as mostly consumed when only 10% or less of fuel-nitrogen compound (i.e., C<sub>2</sub>N<sub>2</sub> or NH<sub>3</sub>) remained. It is in this region that temperatures are sufficiently high to give realistic results. More than 1000 separate computations were made, for each of many flames (with various  $\phi$  values, fuel-N, and fuel types), in correlation of the  $k$  values. Rates vary substantially over a wide range of  $\phi$ . The numerical coefficients for  $k_8$  considered all of the numerical values through a curve fit of log rate coefficient vs reciprocal temperature by the least-squares method. The validity of this method has been demonstrated by Chen et al.<sup>19</sup> by independently determining the rate coefficients measured by De Soete<sup>7</sup> for the reactions of HCN with O<sub>2</sub> and NO (eqs 14 and 17).



Simulation conditions:

De Soete<sup>7</sup> cases:  $\phi=1.0$  to  $1.58$ ;

Haynes<sup>38</sup> cases:  $\phi=1.6$  to  $2.08$

Correlation from  $k_{14}$  with  $b=f(X_{O_2})$ :  $\ln k_8 = -0.917 \times 10^4/T + 14.63$

Correlation from  $k_{14}$  with  $b=1.5$ :  $\ln k_8 = -0.951 \times 10^4/T + 14.80$

De Soete's<sup>7</sup>  $k_{14}$ :  $\ln k_8 = -0.89 \times 10^4/T + 14.01$

$\ln k_{17} = 27.7 - 2.95 \times 10^4/T$

**Figure 6.** Correlations of the global reburning NO rate constants from the simulations of fuel-N ( $C_2N_2$ ) containing flames.

The expression for  $k_8$ , determined from eq 21, is

$$k_8 = \frac{r_8}{X_{HC}X_{NO}} = \frac{k_{14}X_{HCN}X_{O_2}^b - (dX_{NO}/dt) - k_{17}X_{HCN}X_{NO}}{X_{HC}X_{NO}} \quad (24)$$

where  $b$  is the function of the oxygen concentration given by De Soete<sup>7</sup> and  $X_{HC}$  is the sum of all hydrocarbon radical and hydrocarbon species concentrations. In eq 24,  $k_8$  is a function of  $k_{14}$ , and hence comparisons of  $k_8$  with different  $k_{14}$  expressions by De Soete<sup>7</sup> are also given. Three correlations of the global reburning-NO rate expression were obtained for  $CH_4$  and  $C_2H_4$  flames from the method of this study, as shown in Figure 6. Two  $k_8$  values were obtained from values of  $k_{14}$  derived from simulations<sup>19</sup> with different  $b$  values, and the third is the  $k_8$  value obtained using De Soete's experimental work for  $k_{14}$ .<sup>7</sup> These rate constants can be expressed as below:

$$b = f(X_{O_2}) \quad k_8 = 2.26 \times 10^6 \exp(-18220/RT) \quad (25)$$

$$b = 1.5 \quad k_8 = 2.68 \times 10^6 \exp(-18900/RT) \quad (26)$$

$$\text{exptl } k_{14} \quad k_8 = 1.22 \times 10^6 \exp(-17684/RT) \quad (27)$$

The correlated rate constants from  $b = 1.5$  and  $b = f(X_{O_2})$  show only a small difference, which means that the global reburning rate constants are not very dependent on the oxygen concentration in these flames. The  $k_8$  rate based on the simulated  $k_{14}$  (from this study) is higher than  $k_8$  based on the experimental  $k_{14}$  (from De Soete<sup>7</sup>). As pointed out earlier, without having considered the reburning process in its derivation, the  $k_{14}$  value determined by De Soete may lead to low values of  $k_8$ .

The  $k_8$  correlations by eq 24 with NO-seeded flames can be expressed as

$$b = f(X_{O_2}) \quad k_8 = 5.14 \times 10^5 \exp(-18880/RT) \quad (28)$$

and

$$b = 1.5 \quad k_8 = 4.9 \times 10^5 \exp(-18200/RT) \quad (29)$$

and

$$\text{exptl } k_{14} \quad k_8 = 4.4 \times 10^5 \exp(-17700/RT) \quad (30)$$

The  $k_8$  rates correlated from the flames with NO seeding are illustrated in Figure 7. When NO seeding is used, the reburning-NO mechanism is dominant, and the formation of NO through the fuel-N pathway is

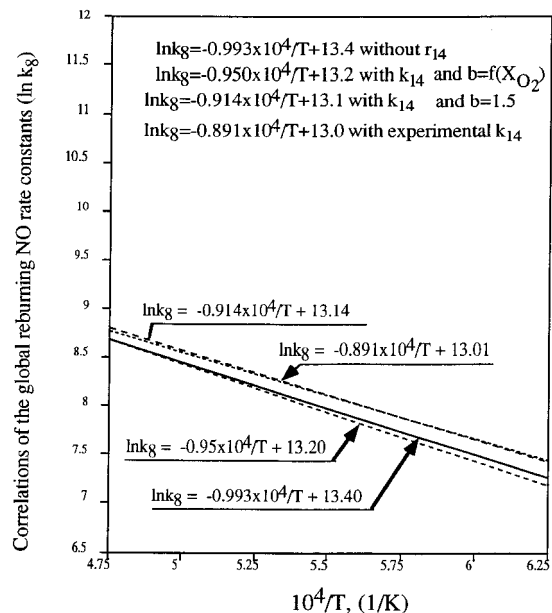


**Figure 7.** Correlations of the global reburning NO rate constants by the simulations with NO seeding in the flames ( $A_8$  and  $E_8$ ).

thought to be less important. Therefore, a second correlative equation without  $k_{14}$  can be written as follows:

$$k_8 = -[(dX_{NO}/dt) - r_{17}]/X_{HC}X_{NO} \quad (31)$$

Correlation for  $k_8$  by eq 31 from the flames with NO seeding and without  $k_{14}$  is

$$k_8 = 6.6 \times 10^5 \exp(-19700/RT) \quad (32)$$

The global activation energies from the seven expressions for  $k_8$  (eqs 25–30 and 32) are within  $\pm 6\%$  of the average value, and the pre-exponential factors are within a factor of 2.5 of the average value. The global reburning rate with NO seeding exhibits lower values compared to those without NO seeding.

The magnitude of the activation energy for the global rate constant  $k_8$  determined from simulations is consistent with values estimated from the governing elementary kinetic steps used in these simulations.<sup>17,35</sup> The cumulative activation energy from the elementary chemical steps falls in the range of 15 000–20 000 cal/gmol, and the correlated activation energy ( $E_8 \sim 18$  000 cal/gmol) is within this range. The significance of the global reburning-NO pathway can also be illustrated by the ratio of the global rates  $r_8$  vs  $r_{17}$  (Figure 8). Under fuel-lean conditions, the ratio is much less than unity,

(35) Tsang, W.; Hampson, R. F. Chemical kinetic data base for combustion chemistry: Part 1. Methane and related compounds. *J. Phys. Chem. Ref. Data* **1986**, *15*, 3.

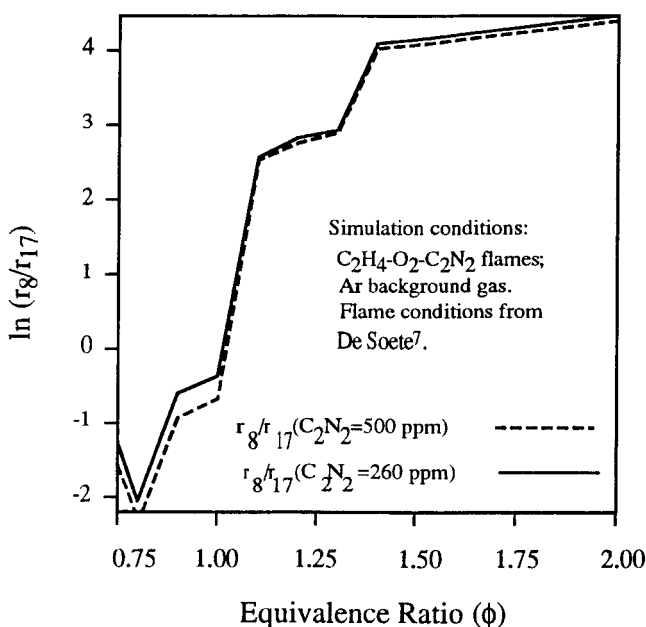


**Figure 8.** Global rate ratio of  $r_8/r_{17}$  for premixed  $C_2H_4/O_2$  flames calculated from the comprehensive elementary step reaction sequence.

which indicates that the reburning mechanism is not dominant in the reduction of NO. With the increase of equivalence ratio, the global reburning rate is higher than the  $HCN + NO \rightarrow N_2$  global rate by 3 or 4 orders of magnitude. In these fuel-rich flames, the reburning-NO pathway is the major NO reduction mechanism. Fuel-N levels also slightly change the ratio of the reaction rates; a higher fuel-N concentration ( $C_2N_2 = 500 \text{ ppm}$ ) yields a slightly lower rate ratio.

Further evaluation of  $k_8$  in predicting NO concentrations in fuel-rich, turbulent diffusion flames is addressed in another paper,<sup>36</sup> where measured and predicted NO values are compared to measurements from practical, staged, and reburning flames. In these computations, the proposed global NO sequence of Figure 2 has been integrated into a generalized, comprehensive combustion model, pulverized coal gasification and combustion in three dimensions (PCGC-3).<sup>29</sup> The global reburning-NO pathway is included and is shown to be important when fuel-rich flames or NO-seeded flames are encountered. The simulations also show that when fuel-N exists ( $>100 \text{ ppm}$ ), thermal-NO and prompt-NO may be negligible ( $<5\%$ ).

The  $k_8$  rate expression recommended for a global  $NO_x$  kinetic model, which is a composite of eqs 25–30 and 32, is

$$k_8 = [(2.7 \pm 0.15) \times 10^6] \exp[(-18800 \pm 500)/RT] \quad (33)$$

where uncertainty levels were estimated from differences between specific predicted rate constant values for each point in the computed flames and the correlated value (see Figure 4.17 of ref 20).

### Summary and Conclusions

Reburning is a relatively new industrial process, whereby a hydrocarbon fuel such as natural gas is added

downstream of the flame zone to reduce NO to HCN and eventually to  $N_2$ . It is also an important chemical step in a reacting, fuel-rich mixture. However, while fundamental predictions in laminar flames with comprehensive kinetic mechanisms can be performed, no global rate expression for the reburning reaction,  $\sum_i C_i H_j + NO \rightarrow HCN + \dots$ , has been reported for use in turbulent, diffusion flames. This paper reports the rate parameters for this reaction over a range of equivalence ratios (1.0–2.08) at atmospheric pressure. Simulations of several premixed hydrocarbon flames were performed with CHEMKIN to provide a comprehensive set of radicals, intermediates, and major species profiles. Thermal-NO and prompt-NO were neglected in the presence of fuel-N and in fuel-rich systems. A global rate expression for the reburning reaction was postulated, and the associated rate constant,  $k_8$ , was determined for different combustion conditions from the simulated radical, intermediate, and major species profiles in premixed, laminar flames.

Various techniques were used to evaluate the global reburning-NO rate expression. These include comparison of data correlations from several different flames, comparison to the elementary chemical steps, and verification of the trends with findings from other investigators. The results from these techniques show a qualitative consistency with the global reburning-NO rate expression. The rate constants correlated from the simulated flames with or without NO seeding also show good agreement. The quantitative evaluation of this new global rate expression and its parameters by comparison with the data from turbulent, particle-laden diffusion flames with reburning is treated in another paper.<sup>36</sup>

### Nomenclature

PCGC-3 = pulverized coal gasification combustion, three-dimensional computer code

CHEMKIN = CHEMical KINetic computer program

$b$  = exponential factor for oxygen concentration determined by De Soete<sup>7</sup>

$C_i$ , various units = concentration of species  $i$

HC = hydrocarbon

$C_i H_j$  = hydrocarbon

$k_j$ ,  $\text{gmol cm}^{-3} \text{s}^{-1}$  = rate constant of reaction  $j$

$M$  = third body in a chemical reaction

$r_i$ ,  $\text{gmol cm}^{-3} \text{s}^{-1}$  = global rate of the pathway  $i$

$R$ ,  $\text{kcal kg mol}^{-1} \text{K}^{-1}$  = ideal gas constant

$T$ , K = temperature

$t$ , s or ms = time

$X_i$  = mole fraction of species  $i$  in the gas phase

$\phi$  = equivalence ratio

**Acknowledgment.** This research was sponsored by the Advanced Combustion Engineering Research Center. Funds for this center are received from the National Science Foundation (Engineering Education and Centers Division), the State of Utah (Centers of Excellence), 37 industrial participants, the U.S. Department of Energy, NASA, and the Environmental Protection Agency. The work of Mrs. Eva Black in finalizing the manuscript and of Miss Jan Stieff with the figures is appreciated.

EF960007V

(36) Smoot, L. D.; Hill, S. C.; Xu, H.  $NO_x$  control through reburning. *Prog. Energy Combust. Sci.* **1996**, submitted for publication.

(37) Haynes, B. S. The oxidation of hydrogen cyanide in fuel-rich flames. *Combust. Flame* **1977**, 28, 81.

(38) Haynes, B. S. Reactions of ammonia and nitric oxide in the burnt gases of fuel-rich hydrocarbon-air flames. *Combust. Flame* **1977**, 28, 113.